Wide-Field Infrared Survey Telescope (WFIRST): Composite Structure Verification for Operational Temperatures

James Mondello[a], Paul Baird[b], Lisa Bartusek[b], David Content[b], Robert Egerman[a], Joseph Marzouk[b], Bonnie Patterson[a], Thomas Quinzi[a], Benjamin Rodini[b], Cory Smiley[a], J. Scott Smith[b]

[a]Harris, Rochester NY; [b]NASA Goddard Space Flight Center, Greenbelt MD

ABSTRACT

The Wide-Field Infrared Survey Telescope (WFIRST) mission is the next large astrophysics observatory for NASA after the James Webb Space Telescope and is the top priority mission from the 2010 National Academy of Sciences' decadal survey. The WFIRST Optical Telescope Assembly (OTA) includes inherited composite support structures that were originally designed and tested for room temperature operation; however, the WFIRST mission will require operation at colder temperatures to achieve sufficient sensitivity for the infrared wavelengths. We will present the results and conclusions of testing completed at the coupon and engineering model level to verify that the inherited composite structures will maintain mechanical integrity and performance over the required temperature range. The testing included: (1) characterization testing of constituent material coupons, (2) thermal cycling and static load testing of a representative aft metering structure (AMS) and forward metering structure (FMS), and (3) thermal cycling and dynamic testing of a representative secondary mirror assembly (SMA).

Keywords: WFIRST, composite, metering, structures, telescope

1. INTRODUCTION

The WFIRST mission leverages a repurposed, space-flight-qualified 2.4-meter, obscured two-mirror telescope, modified to include the addition of a tertiary mirror (for the wide-field instrument) to create a three-mirror anastigmatic optical configuration and achieve wide field of view (FOV) capability[1-3]. The repurposed components of the optical telescope assembly (OTA) are shown in Figure 1 and include the aft metering structure (AMS), forward metering structure (FMS), secondary mirror support structure (SMSS), and secondary mirror support tubes (SMSTs), which together form the forward optical assembly (FOA) portion of the telescope.
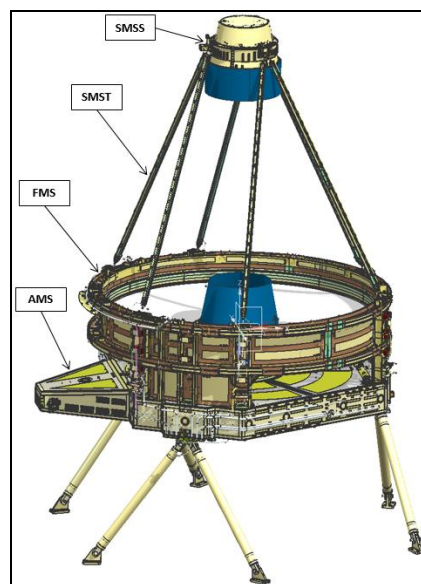

Figure 1: AMS, FMS, SMST, and SMSS hardware will be repurposed for the WFIRST mission

The FOA structures consist primarily of composite materials composed of high-modulus fibers in a hygroscopically stable cyanate siloxane resin matrix to allow for stability, strength, and stiffness optimization at a low weight. During fabrication, tight control of prepreg properties, ply orientations, fiber volume, and cure cycle parameters was maintained to minimize coefficient of thermal expansion (CTE) variability. In some regions, honeycomb panels composed of inner and outer composite facesheets with an aluminum honeycomb core were used. Within the composite structures, metallic interface fittings were bonded in place using a two-part epoxy adhesive chosen for its high shear and peel strengths at room temperature, along with good workability characteristics.

These composite structures were originally designed, developed, built, and tested by Harris (formerly Exelis, ITT, Kodak) for room temperature operation circa 2000-2004. To enhance the infrared science performance of WFIRST, the FOA structures are being repurposed to operate at less than 270K[1]. This paper describes the activities performed to verify that the inherited composite structures will maintain mechanical integrity during and after exposure to this temperature, as well as retain stability performance over the required temperature range.

2. CHARACTERIZATION TESTING

A comprehensive suite of mechanical characterization testing was conducted to (1) understand the impact of temperature on the material properties, and (2) verify aging of the hardware did not result in any changes to CTE.

2.1 Coefficient of Thermal Expansion Coupon Testing

CTE coupon testing was performed as part of early operational temperature studies to mitigate risk. CTE coupons from the original build of the FOA structures have been retained and maintained in controlled storage. Room temperature CTE tests on the heritage coupons were re-performed at Harris using the same methodology (a precision dilatomer) to understand if there were any changes due to composite aging. The CTE values from the re-test performed in 2014 were compared to the original test values from 2001-2002, and the results are shown in Figure 2. For all coupons tested, there was no statistical difference between the re-tested and original values, and all differences were within measurement uncertainty. The outcome of this testing demonstrated that the composite materials used in the repurposed hardware retained their stability-critical CTE performance over time during storage.
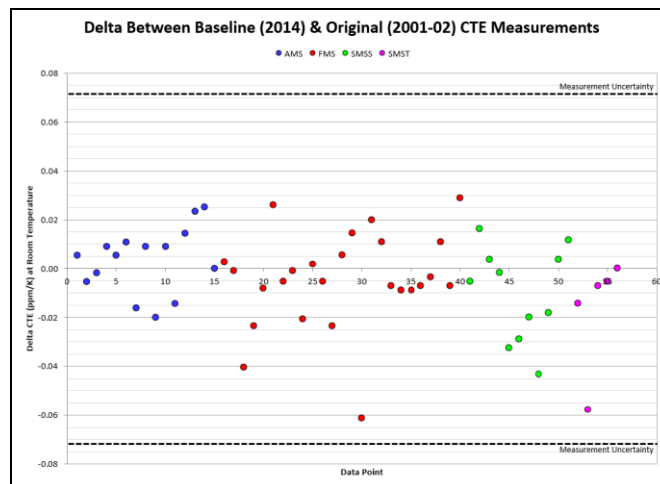

Figure 2. Retesting of original CTE coupons at room temperature demonstrated that there was no statistical change due to material aging (within measurement uncertainty)

After completion of room temperature CTE testing, the heritage coupons were then CTE tested over an extended temperature range. The results were compared to the room temperature values, along with original design acceptance ranges, which are typically used as a basis for Monte Carlo analyses used to verify FOA optical performance. For the carbon-reinforced composite laminates tested, the CTE was relatively insensitive to temperature over the range tested, and values were within original design acceptance ranges. A typical plot of CTE versus temperature is shown in Figure 3. The one exception was for a boron/carbon-reinforced composite laminate, with CTE decreasing more significantly at

colder temperatures, as shown in Figure 4. This was not an unexpected result based on the presence of the non-carbon-based fiber in this laminate and its behavior with temperature.
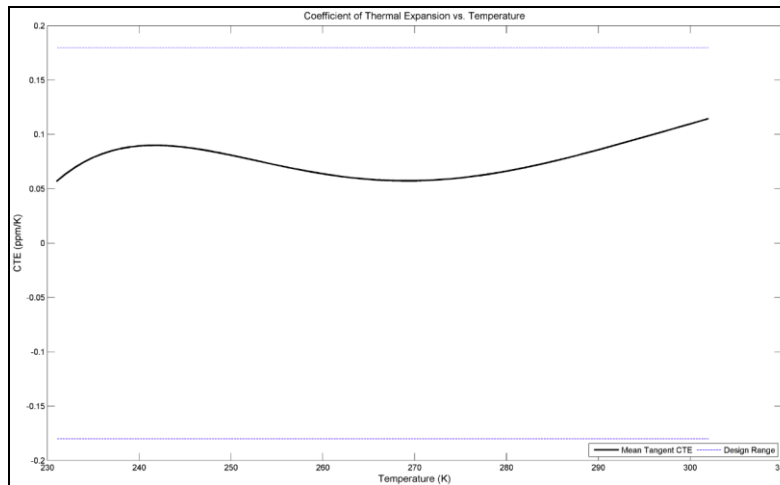

Figure 3. CTE of carbon fiber reinforced composite materials showed insensitivity to temperature change over the tested range and were within original design acceptance criteria
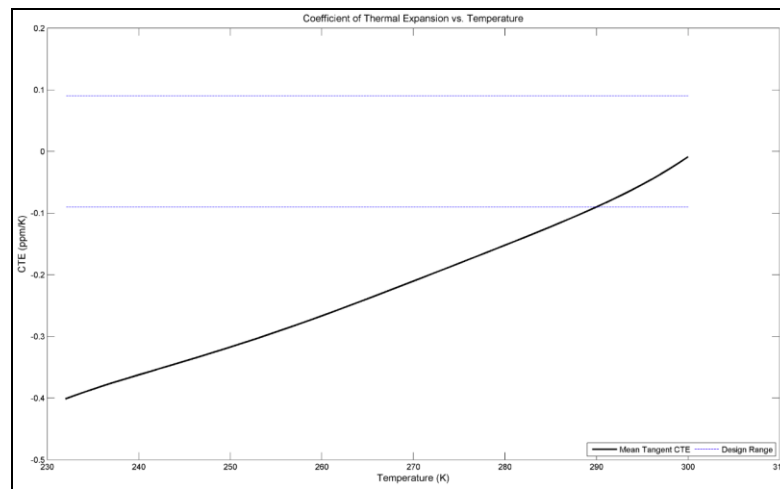

Figure 4. CTE of boron/carbon fiber reinforced composite material showed higher sensitivity to temperature change over the tested range

2.2 Tensile Coupon Testing

During operational temperature studies, tensile testing was also performed to assess the impact of thermal cycling on tensile strength. Heritage CTE coupons from the original build of the FOA structures were also utilized for this activity with modifications to allow for tensile testing. For each composite laminate type, samples were tensile tested at room temperature without thermal preconditioning to form a baseline and were compared to samples tensile tested after thermal cycling. A comparison of thermal cycled to uncycled tensile strengths is shown in Figure 5. While some variation was seen, there was no statistical difference observed due to thermal cycling of the coupons. These results verified that room temperature tensile properties of the composite laminates were not altered due to thermal cycling.
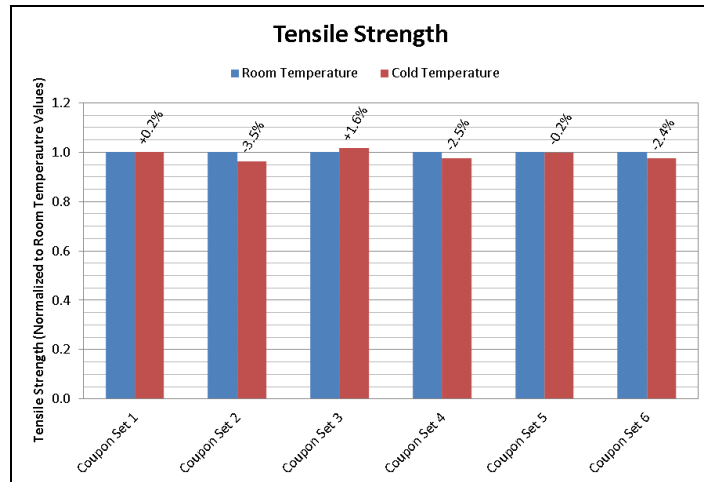
Figure 5. No statistical difference was observed in tensile strength due to thermal cycling of the coupons

2.3 Material Property Characterization

After completion of the smaller scale risk mitigation coupon activities described in sections 2.1 and 2.2, a full suite of mechanical testing was performed to determine key material properties at cold temperature to use in analytical assessment of thermal loads. The material properties were tested for each unique constituent material within the FOA composite structures, which consisted of eight lamina, eleven laminates, two honeycomb panels, and two adhesives.

To ensure consistency with the original composite material, prepreg was procured to the same specifications using the same supplier. For each set of panels, room temperature acceptance testing (CTE, fiber volume, 0° short beam shear) was conducted prior to any cold temperature testing to verify that the panels met the requirements of the original hardware and provided representative data. For adhesive samples, single lap witness coupons were bonded for each mix and tested at room temperature for workmanship. Harris standard processes and procedures consistent with the original build, along with ASTM standards, were used to fabricate all samples.

The suite of mechanical testing performed consisted of sixteen unique test methods, and over 1900 total coupons tested at the Harris environmental test facilities, including both cold property and ambient acceptance testing. Table 1, Table 2, and Table 3 list the tests conducted for lamina/laminates, honeycomb panels, and adhesives, respectively.

Table 1. Test types and related standards for lamina and laminate materials

Description	Test Specification
Tensile Modulus, Strength, Poisson's Ratio (0°/90°)	ASTM D3039
Compression Modulus (0°/90°)	SACMA SRM 1R-94
Compression Strength (0°/90°)	SACMA SRM 1R-94
Short Beam Shear Strength (0°/90°)	ASTM D2344
Iosipescu (V-Notch) Shear Strength, Modulus	ASTM D5379
Flatwise Tensile Strength	ASTM D7291 (Mod)
Fiber Volume / Void Content	ASTM D3171/D2734
CTE (over temperature range)	ASTM E289
CTE (at room temperature)	Harris Procedure

Table 2. Test types and related standards for honeycomb panel materials

Description	Test Specification
Flatwise Tensile Strength	ASTM C297
Flatwise Compressive Modulus, Strength	ASTM D365
Core Shear (0°/90°)	ASTM C273
CTE (over temperature range)	ASTM E289
CTE (at room temperature)	Harris Procedure

Table 3. Test types and related standards for adhesive materials

Description	Test Specification
Tensile Modulus, Strength, Poisson's Ratio	ASTM D638
Compression Strength	ASTM D695
Iosipescu (V-Notch) Shear Strength, Modulus	ASTM D5379
Flatwise Tensile Strength	ASTM D7291 (Mod)
Thick Adherend Stress Strain	ASTM D5656
Double Lap Shear	ASTM D3528
Single Lap Shear	ASTM D1002
CTE (over temperature range)	ASTM E289
CTE (at room temperature)	Harris Procedure

All coupons were thermally conditioned prior to cold testing by exposing them to multiple thermal cycles over the temperature range in a controlled environmental chamber. A representative coupon for each material was instrumented with a thermocouple and monitored during the thermal cycle for validation.

A majority of the laminate mechanical test results fell within ±15% of room temperature values, demonstrating robustness to the WFIRST operating environment. As an example, a comparison of cold temperature tensile modulus and compression modulus to room temperature values is shown in Figure 6. CTE variation over temperature was minimal, reinforcing the results observed during earlier coupon testing described in Section 2.1.
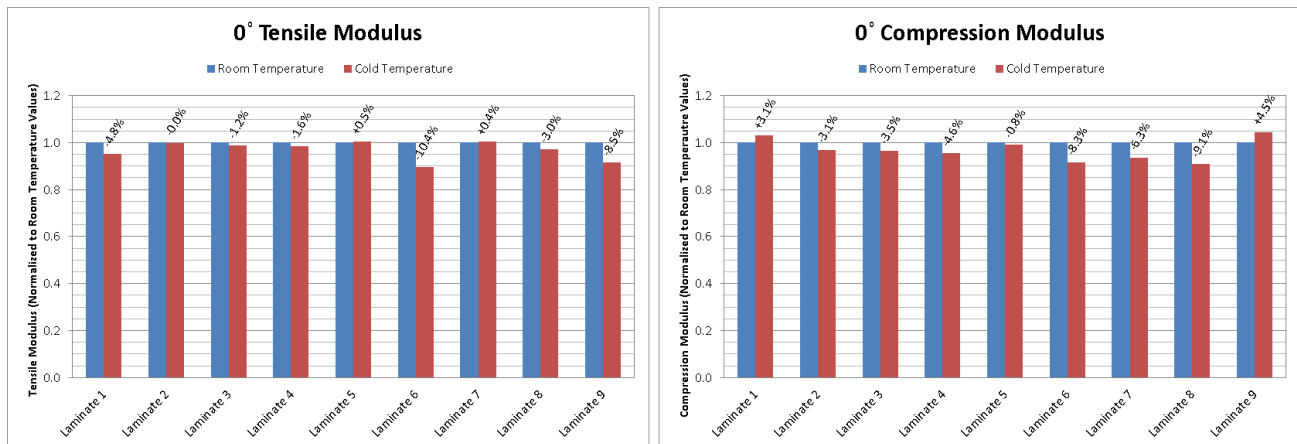

Figure 6. Laminate mechanical test results were typically in-family with room temperature values within ±15%

Adhesive mechanical test results were also generally consistent with expected adhesive behavior at cold temperature (increased modulus/strength, decreased plasticity, CTE variation with temperature). For most of composite-to-metal configurations, the double lap shear strength at cold temperature was degraded. The degree of degradation was configuration-specific and dependent upon the stiffness of the outer ply in the composite laminate; composites with stiffer outer plies demonstrated more degradation with cold temperature. Additionally, samples tested with thicker composite adherends were more susceptible to peel-induced failure, as was seen by the decrease in peak load for those configurations.

The data collected during the material development activity were reduced to develop temperature dependent property sets for finite element models. B-basis allowables were generated for the composite materials to enable ply-by-ply and homogeneous laminate thermal margin assessments. B-basis allowables were also generated for the adhesive joint configurations using Hart-Smith[4] methodologies to enable bond thermal margin assessments.

3.   DEVELOPMENT ARTICLE TESTING

Leveraging the material properties and allowables generated from the coupon characterization testing, detailed finite element models were evaluated to assess the safety of the FOA structures. Although analytical assessment of the structures indicated that the repurposed hardware would survive the thermal extremes, we felt it was necessary to demonstrate survival empirically through physical testing of representative hardware. During the original hardware build, engineering models of the AMS, FMS, and SMSS were fabricated and assembled as pathfinder development articles and had been maintained in controlled storage. As part of this activity, the development articles were thermal cycled and load tested. The goal of the development article testing was to demonstrate survivability of the hardware at the temperature extremes as the prime hardware will need to withstand launch loads after being exposed to thermal cycles during ground testing.

3.1 Aft Metering Structure and Forward Metering Structure

The AMS and FMS development articles are full-sized 120° segments of the prime hardware and contain representative bond geometries and material types. The development articles were fabricated and assembled during the original hardware build using consistent processes, and are representative of material aging and workmanship contained in the prime hardware. A CAD depiction of the development articles is shown in Figure 7.
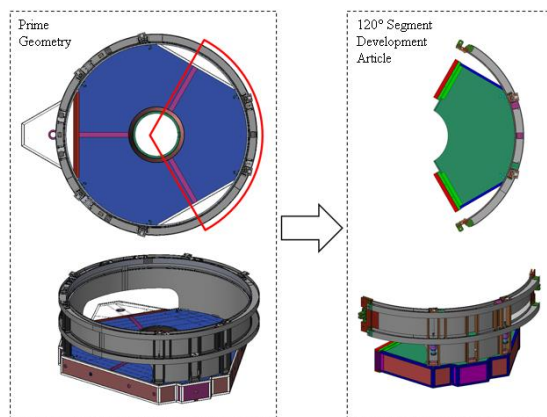

Figure 7. AMS and FMS development articles are full-size 120° segments representative of the prime hardware

The test sequence consisted of the following three activities: baseline static load test (SLT), thermal cycling, and post-thermal-cycle SLT. Between each of the test activities, all accessible bonds of the hardware were thoroughly examined using ultrasonic inspection techniques to verify that there were no indications of structural failure.

The baseline SLT was conducted to demonstrate structural integrity of the development hardware after previously observed environmental conditions and approximately fourteen years in storage. Additionally, the baseline SLT was used to obtain strain and deflection data for comparison of structural behavior before and after thermal cycling. During the static load testing, ten load cases were simulated in the structures to provide representative loading conditions in the bonds with the lowest thermal margins. The test was performed in the Harris environmental test facility SLT tower and utilized nineteen hydraulic actuators to apply interface and body loads. The AMS and FMS were instrumented with thirty-five single axis strain gages, eighteen tri-axis rosette strain gages, six linear variable differential transformers (LVDTs), and twenty-six acoustic emission (AE) sensors to monitor the real-time test behavior. The test configuration is shown in Figure 8.

Figure 8. The AMS/FMS static load testing was conducted in the Harris environmental test facility SLT tower and utilized nineteen actuators to apply interface and body loads

The measured strain data from the baseline SLT were compiled and compared to finite element (FE) predictions. Good correlation was observed between measured strain values and FE predicted strain values for all load cases, indicating that the model was a valid representation of the hardware. To determine the level of correlation, measured values were plotted against predicted values, and a linear least-squares regression line was fit to the data. The regression line was forced through the origin, and the resulting slope and R^2 parameters were used together to describe the correlation of the data. The slope of the regression line provides a metric to evaluate how well the average measured values matched the average predicted values. For a perfect correlation, the slope of the regression line would be 1. The R^2 value (coefficient of determination) provides a metric to evaluate how much scatter there is around the fitted regression line. A regression line that perfectly describes the test data would have an R^2 value of 1. An example of the measured-to-predicted strain for a baseline load case is shown Figure 9.
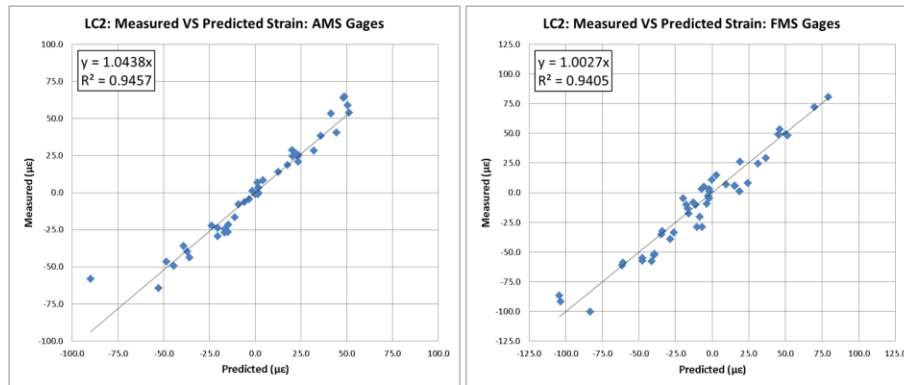

Figure 9. Good correlation was observed between measured and FE predicted strain for the AMS and FMS

Linear relationships were observed for strain versus load and deflection versus load for all load cases, indicating that a structural failure did not occur during any load case. Symmetric behavior was observed in the structures for symmetric load cases, offering additional evidence that no structural failure occurred prior to, or during testing. No anomalous acoustic activity was observed, and the quantity and nature of AE activity observed throughout the test was consistent with a robust structural assembly. Finally, ultrasonic inspections performed before and after the baseline SLT were consistent and did not provide any evidence of structural failures.

After completion of the baseline SLT, the AMS and FMS development articles were thermal cycled in an air-controlled chamber. The hardware was cycled between 253K and 311K for multiple iterations to envelope the potential operational temperature range with additional margin. To monitor the part temperatures in situ and accurately control ramp rates

and dwell times, thirty-nine thermocouples were located on the metallic fittings and composite panels of the AMS and FMS as shown in Figure 10.
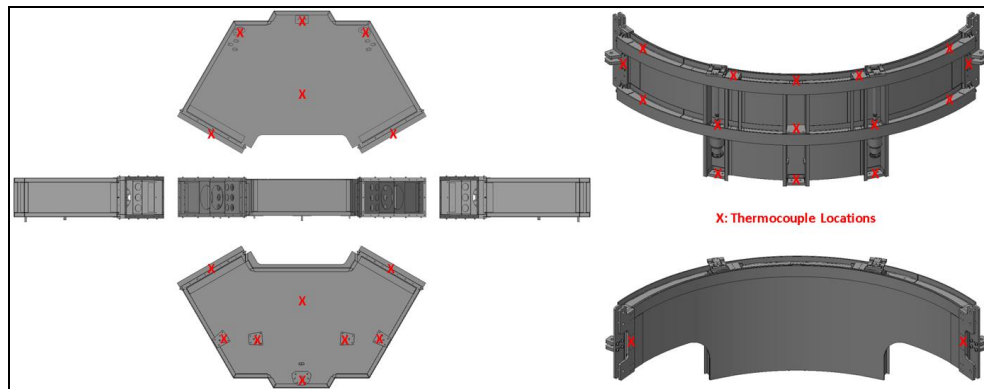

Figure 10. Thirty-nine thermocouples were located on the AMS and FMS development articles to monitor hardware temperature in situ

Ultrasonic inspections performed before and after the thermal cycles were consistent and did not provide any evidence of structural failures.

After completion of thermal cycling, the AMS and FMS development articles were re-configured in the Harris environmental test facility SLT tower, as shown in Figure 8. All instrumentation remained in the same locations on the hardware, and the same load cases from the baseline SLT were repeated for the post-thermal-cycle SLT.

For this testing, the measured strain data from the post-thermal-cycle SLT were compared to the measured strain data from the baseline (pre-thermal-cycle) SLT. Excellent correlation was observed between the post-thermal-cycle SLT and baseline SLT measured strain for all load cases, demonstrating that the thermal cycles did not alter or damage the structures. The post-thermal-cycle versus baseline AMS and FMS strain data, compiled for all load cases, is shown in Figure 11.
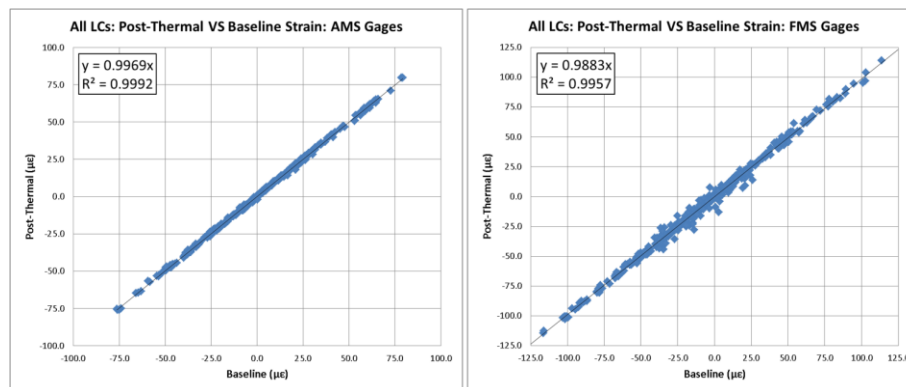

Figure 11. Excellent correlation was observed between post-thermal-cycle and baseline strain for the AMS and FMS

As with the baseline SLT, linear relationships were observed for strain versus load and deflection versus load for all load cases, indicating that a structural failure did not occur during any load case. Symmetric behavior was observed in the structures for symmetric load cases, offering additional evidence that no structural failure occurred prior to, or during testing. No anomalous acoustic activity was observed, and the quantity and nature of AE activity observed throughout the test was consistent with a robust structural assembly. Finally, ultrasonic inspections performed before and after the post-thermal-cycle SLT were consistent and did not provide any evidence of structural failures.

The post-thermal-cycle SLT demonstrated that the representative AMS and FMS development structures are capable of withstanding representative loads after being subjected to thermal cycling, and the excellent correlation of structural behavior during the baseline SLT and post-thermal-cycle SLT verified that structural integrity is maintained during exposure to potential temperature extremes.

3.2 Secondary Mirror Support Structure

The SMSS development article is a full-sized prime-like structure and contains representative bond geometries and material types. The development article was fabricated and assembled during the original hardware build using consistent processes, and is representative of material aging and workmanship contained in the prime hardware. For this testing, the SMSS was assembled with aluminum mass simulators of the mirror and actuators to form the development secondary mirror assembly (SMA) article. A CAD depiction of the development article is shown in Figure 12.
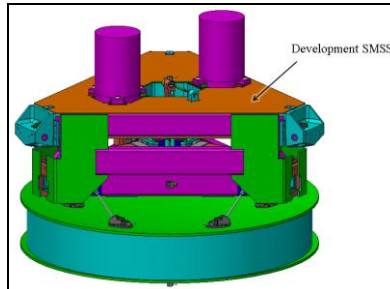

Figure 12. SMSS development article is a full-size structure representative of the prime hardware

The test sequence was very similar to that performed on the AMS and FMS development articles described in Section 3.1, except dynamic testing was performed on the SMA development article. The test sequence consisted of the following three activities: baseline random vibration test, thermal cycling, and post-thermal-cycle random vibration test. Between each of the test activities, all accessible bonds of the hardware were thoroughly examined using ultrasonic inspection techniques to verify that there were no indications of structural failure.

The baseline random vibration test was conducted to demonstrate structural integrity of the development hardware after previously observed environmental conditions and approximately fourteen years in storage. Additionally, the baseline test was used to obtain dynamic response signatures for comparison of structural behavior before and after thermal cycling. The random vibration testing was performed in three axes with multiple load increments. Low-level vibration surveys were performed before and after the full-level test sequence for each axis to verify no structural changes occurred. The test was performed using the Harris environmental test facility MB C210 shaker system. The test instrumentation consisted of fifteen triaxial accelerometers, with three control accelerometers located on the fixture and twelve response accelerometers located on the SMA development article. The SMA was supported on the shaker using flexures to simulate the stiffness of the SMSTs. The test configuration is shown in Figure 13. During each test, frequency response function (FRF) plots were generated for each response accelerometer using the excitation axis of a fixture accelerometer as the reference. FRF plots from each portion of the test sequence were overlaid and compared to one another to look for any frequency shifts that could indicate structural failure, focusing on the in-axis responses (i.e., the accelerometer axis corresponding to the test excitation axis).
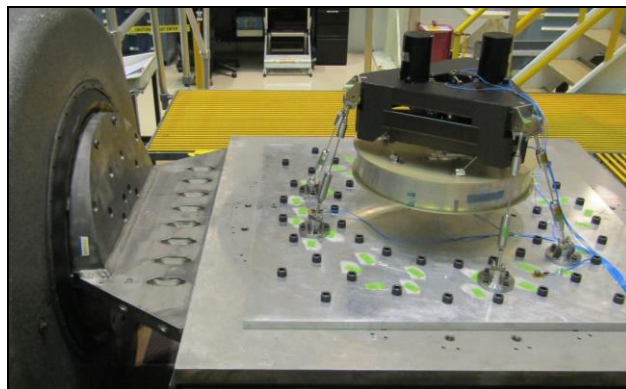

Figure 13. The SMA random vibration testing was conducted using the Harris environmental test facility MB C210 shaker system and was instrumented with fifteen triaxial accelerometers

The FRF plots generated during the baseline random vibration test were overlaid and compared to FRF plots predicted by the FE model using visual inspection of the overlay as well as numerical comparison of frequencies for primary modes that demonstrate significant mass participation in the model. Strong correlation was observed between the response signatures, and most primary modes were within 3%, especially lower frequency modes, indicating that the model was a valid representation of the hardware. An example of the model-to-baseline test FRF overlay is shown in Figure 14.
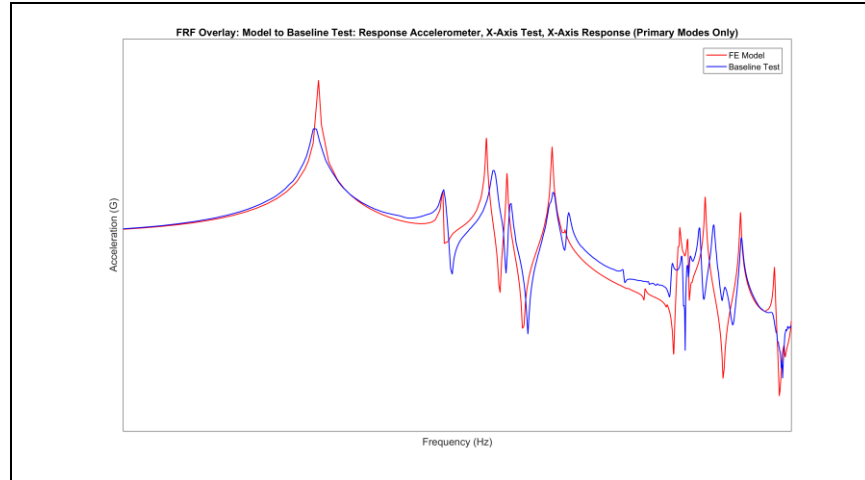

Figure 14. Strong correlation was observed between baseline test and FE model FRF plots, especially for lower frequency modes

FRF plot overlays were also generated for each load level performed during the baseline random vibration testing. Consistent response signatures between load levels were observed for all accelerometers and test axes, indicating linear behavior within the structure and demonstrating that structural integrity did not degrade as load level was increased (shown in Figure 15). Finally, ultrasonic inspections performed before and after the baseline random vibration test were consistent and did not provide any evidence of structural failures.
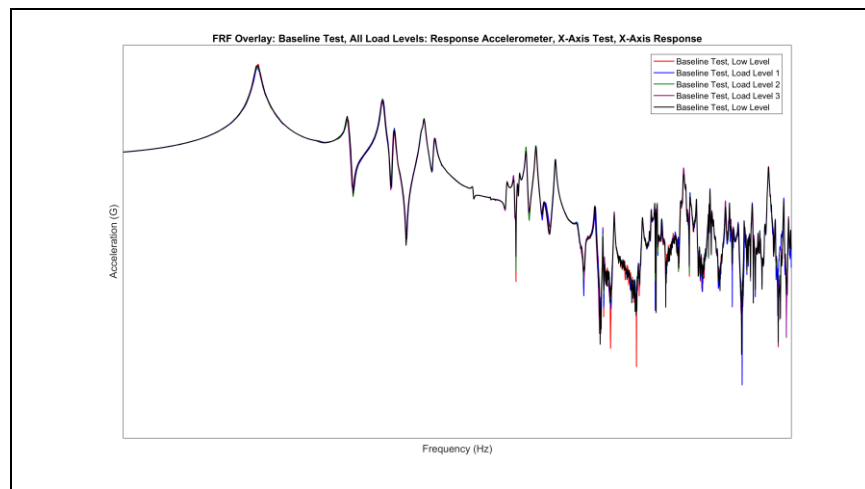

Figure 15. FRF plot overlays were consistent for load levels during the baseline random vibration test

After completion of the baseline random vibration test, the SMA development article was thermal cycled in an air-controlled chamber. The hardware was cycled between 253K and 311K for multiple iterations to envelope the potential operational temperature range with additional margin. To monitor the part temperatures in situ and accurately control ramp rates and dwell times, thirty-five thermocouples were located on the metallic fittings and composite panels of the SMA as shown in Figure 16.
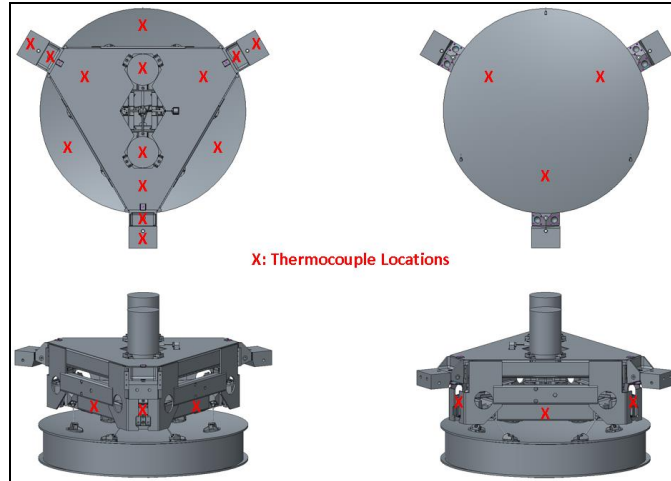
Figure 16. Thirty-five thermocouples were located on the SMA development article to monitor hardware temperature in situ

Ultrasonic inspections performed before and after the thermal cycles were consistent and did not provide any evidence of structural failures.

After completion of thermal cycling, the SMA development article was re-configured on the Harris environmental test facility MB C210 shaker system, as shown in Figure 13. All instrumentation remained in the same locations on the hardware, and the same dynamic load levels from the baseline random vibration test were repeated for the post-thermal-cycle random vibration test.

For this testing, the FRF plots generated on the post-thermal-cycle random vibration test were overlaid and compared to FRF plots generated during the baseline random vibration test; primary mode frequency values were also compared. Excellent correlation was observed between post-thermal-cycle and baseline response signatures for all test axes and accelerometers, and most primary modes were well within 1%. An example of the baseline-to-post-thermal-cycle test FRF overlay is shown in Figure 17.
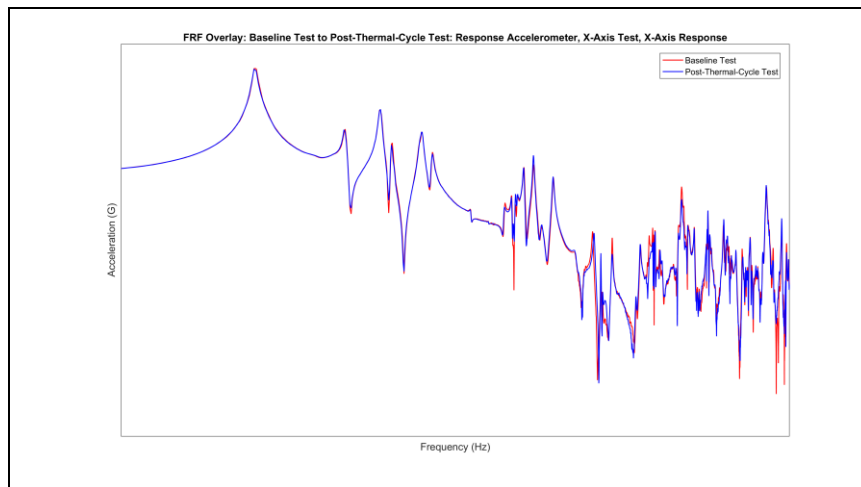

Figure 17. Excellent correlation was observed between post-thermal-cycle test and baseline test FRF plots

As with the baseline random vibration test, consistent response signatures between load levels were observed for all accelerometers and test axes during the post-thermal-cycle random vibration test, indicating linear behavior within the structure and demonstrating that structural integrity did not degrade as load level was increased. Finally, ultrasonic inspections performed before and after the post-thermal-cycle random vibration test were consistent and did not provide any evidence of structural failures.

The post-thermal-cycle random vibration testing demonstrated that the representative SMA development structures are capable of withstanding dynamic loads after being subjected to thermal cycling, and the excellent correlation of response signatures during the baseline and post-thermal-cycle random vibration tests verified that structural integrity is maintained during exposure to potential temperature extremes.

4. SUMMARY

The WFIRST OTA includes inherited composite support structures that were originally designed and tested for room temperature operation; however, the WFIRST mission will require operation at colder temperatures to achieve sufficient sensitivity for the infrared wavelengths. Material characterization testing of coupon samples demonstrated that the CTE performance of the composite laminates was unaltered due to aging of the hardware and that the CTE of carbon-reinforced composite laminates were generally insensitive to temperature over the desired range. Material property sets and B-basis allowables were generated to allow for analytical assessment of the repurposed hardware over the temperature range, and detailed finite element models were evaluated to assess the safety of the FOA structures. Finally, AMS, FMS, and SMSS development articles were thermal cycled and load tested demonstrating that structural integrity will be maintained in the structures after exposure to thermal extremes.

5. ACKNOWLEDGEMENTS

REFERENCES

[1] Content, D., Aaron, K., Abplanalp, L., Anderson, K., Capps, R., et al., "Wide Field Infra-Red Survey Telescope (WFIRST) 2.4-meter Mission Study," Proc. SPIE 8860 (2013)

[2] Casey, T., et. al., "Wide Field Infrared Survey Telescope (WFIRST) Observatory Overview," Proc. SPIE 10698 (2018)

[3] Smith, J. S., et. al., "Wide-Field Infrared Survey Telescope (WFIRST) – Optical Telescope Assembly (OTA) Status," Proc. SPIE 10698 (2018)

[4] Hart-Smith, L. J., "Adhesive-Bonded Double-Lap Joints", NASA CR-112235 (1973)